THE JOURNAL OF PHYSICAL CHEMISTRY B

Article

pubs.acs.org/JPCB

Morphology and Ion-Conductivity of Gelatin−$LiClO_4$ Films: Fractional Diffusion Analysis

Tania Basu, Minakshi Maitra Goswami, T. R. Middya, and Sujata Tarafdar*

Condensed Matter Physics Research Centre, Physics Department, Jadavpur University, Kolkata 700032, India

ABSTRACT: Biopolymers are expected to replace synthetic polymers in the quest for cost-effective, environment friendly, and pollution free technology. We report here a study on gelatin films with different concentrations of lithium perchlorate, which may be a candidate for electrolyte material in solid polymer batteries. Morphology studies and impedance spectroscopy both are done on the same set of samples. We study the microstructure of the film by SEM and try to see if a correlation between impedance spectroscopy results and features of gel morphology can be identified. A network structure is revealed in the SEM images where details of the network parameters appear to depend on the salt fraction. Analysis of the impedance measurements is done using a physically meaningful model based on material properties instead of the usual equivalent circuit formalism, where circuit elements are difficult to interpret. We find that anomalous diffusion of charge carriers plays an important role; this is incorporated through a fractional calculus approach.

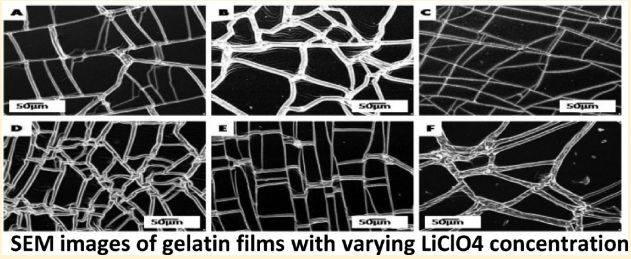

SEM images of gelatin films with varying LiClO4 concentration

1. INTRODUCTION

Polymer electrolytes have been extensively studied for the last two decades.[1−3] Polyethylene oxide is the material used in most of these works. In more recent times, the focus is shifting toward environment-friendly biopolymers, e.g., starch, chitosan, gelatin, etc.[4−7] The most popular salt used for supplying charge carriers in the polymer host is $LiClO_4$;[1,3,8−10] other Li salts are also used.[11] In the present paper, we report work on a film consisting of gelatin, glycerol, formaldehyde, and $LiClO_4$, with different fractions of the lithium salt, and study the morphology by SEM and ion-conductivity by impedance spectroscopy. We study the range between 0 and 17 wt % of salt; here we find that the dc ion-conductivity varies with salt fraction. There is an initial increase of nearly 2 orders of magnitude and then a decrease followed by a more prominent peak at 12.5 wt %. This is similar to double peaks observed in several such materials,[12,13] and the present work offers a justification for this feature. The SEM images reveal interesting network patterns with changes in the details of the structure as the salt fraction varies. For salt concentrations more than 12.5 wt %, SEM images show that the salt does not "dissolve" completely in the host polymer and remains as flower-shaped aggregates scattered on the gelatin network.

A detailed analysis of the SEM images is expected to help in understanding the correlation between morphology and ion-conductivity. At present, we show a qualitative correlation, but further work in this direction may pave the way for better theories explaining the ion-conduction mechanism in complex materials.

In the present paper, we analyze the results on the basis of a model proposed by Lenzi et al.[14] which incorporates anomalous diffusion through a fractional order diffusion equation. The usual procedure is to construct an equivalent circuit which reproduces the impedance results best. However, such an equivalent circuit with lumped circuit elements is often inadequate to explain the behavior of complex materials and distributed elements are introduced in the form of constant phase elements (CPE). The resulting equivalent circuit often has a considerable number of free parameters, and it is difficult to interpret the physical significance of the elements. It has been shown that introduction of a fractional diffusion equation is equivalent to using a CPE[15] and that anomalous diffusion can be modeled by fractional differential equations.[16] We employ the technique suggested by Lenzi et al. where the impedance of a material is calculated from a physical model describing drift and diffusion of charge carriers through a material in an electric field. We calculate the real and imaginary parts of the impedance at varying frequency, for different salt fractions, and compare them with our experimental results. The agreement is good, and the few quantities which are used as fitting parameters are physically meaningful quantities related to material properties.

2. MATERIALS AND METHODS

2.1. Sample Preparation. Gelatin films with glycerol as the plasticizer, formaldehyde as the antifungal cross-linking agent, and $LiClO_4$ as the source of charge carriers were prepared with varying weight fractions (x) of the salt. The weight fraction x is defined as follows:

$$x = \frac{\text{mass of salt}}{\text{sum of mass of all the constituents}} \quad (1)$$

Received: June 24, 2012
Revised: August 14, 2012
Published: August 28, 2012

   dx.doi.org/10.1021/jp306205h | J. Phys. Chem. B 2012, 116, 11362−11369

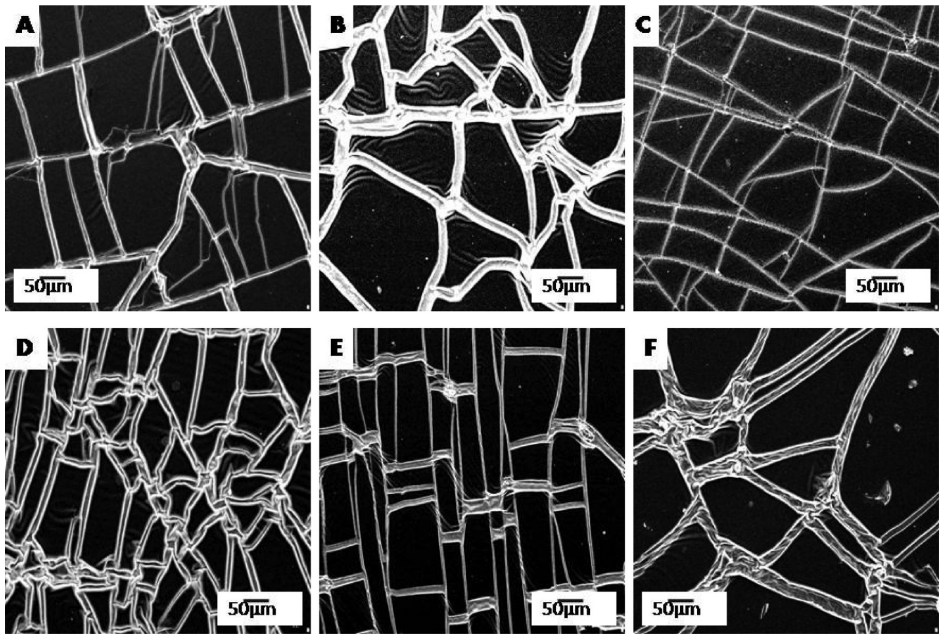

Figure 1. SEM image of gelatin with different wt % of $LiClO_4$: (A) 0.0 wt %; (B) 2.7 wt %; (C) 5.41 wt %; (D) 7.89 wt %, (E) 10.26 wt %, (F) 12.50 wt %.

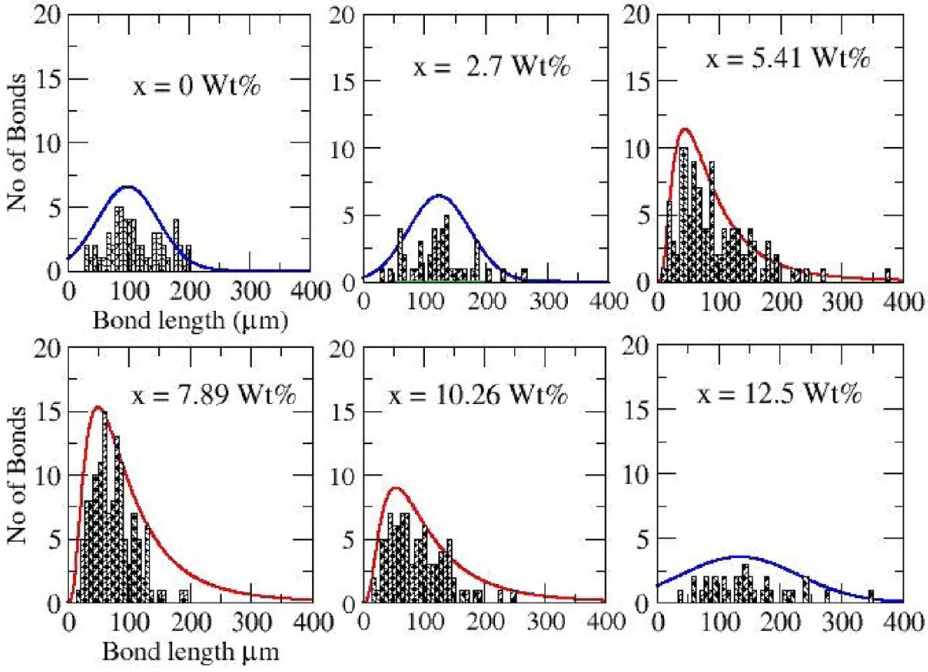

Figure 2. Histogram for bond length distribution with wt % of $LiClO_4$ varying from 0 to 12.50%. For samples with x = 5.41, 7.89, and 10.26 wt %, a log-normal distribution fit is shown (red line). For the other cases, a Gaussian (normal) distribution, shown in blue, gives a better fit.

Transparent films of gelatin (thickness 310−440 μm) are prepared by the solution cast technique.[7] A 2 g portion of commercial gelatin (Merck) was dispersed in 15 mL of distilled water and heated to 50 °C for 25 min under magnetic stirring for complete dissolution. After that, the solution was cooled down to room temperature (30 °C) and 1.25 g of glycerol as plasticizer, 0.25 g of formaldehyde and lithium perchlorate (weight fraction x %) were added to the mixture while stirring for a few minutes. The mass of $LiClO_4$ taken for different samples was 0.1, 0.2, 0.3, 0.4, 0.5, 0.6, and 0.7 g (corresponding to a weight percent of salt of 2.7, 5.41, 7.89, 10.26, 12.5, 14.63, and 16.67%, respectively). Another sample was prepared with no salt but other constituents in the same proportion. This solution was then poured on a Petri dish to form transparent films after drying under vacuum.

2.2. Scanning Electron Microscopy. Scanning electron microscopy (SEM) was done on LEO S 430I (UK) at CGCRI, Kolkata, for all samples for different x at magnifications of 200×.

2.3. Analysis of SEM Images. The SEM images for x up to 12.5 wt % are shown in Figure 1. These images show clear formation of connected networks with a roughly rectangular

dx.doi.org/10.1021/jp306205h | J. Phys. Chem. B 2012, 116, 11362−11369

geometry for all samples. Mostly, we see four strands of the net (which we call bonds) meeting at a node. However, as x increases, the network character changes.

Initially, it becomes less dense with addition of salt, then the density rises and the network has a wider range of bond lengths, and finally for x larger than 10.26%, we again find a less dense network. Here we refer to the distance between successive nodes on the net as "bonds" and the "density" of the network refers loosely to the number density of nodes per unit area in the image. There is apparently no correlation of bond density with the physical density (mass/volume) of the sample, which remains near about 1.2 g/cm^3. To quantify the evolution of the morphology, we use Image Pro Plus software to count the number of bonds of different sizes. The results are plotted in a histogram in Figure 2 for each x. It is seen that for three cases with nonzero x but low conductivity the distribution is log-normal.[17] For the remaining three cases, the distribution is symmetric and a normal (Gaussian) distribution gives a better fit. All the SEM images show network-like structures, but the two images corresponding to x = 2.7 and 12.5 wt % look somewhat different; both have comparatively sparse networks and the total number of bonds at the same magnification is much less. We show later that the dc conductivity is higher for these two samples. It is possible that a denser network makes the structure more rigid and hampers the conduction process. The log-normal distribution with a bias toward shorter bonds is indicative of a denser network.

The images for x = 14.63 and 16.67 wt % are shown in Figure 3. Here the excess salt remains as aggregates of different

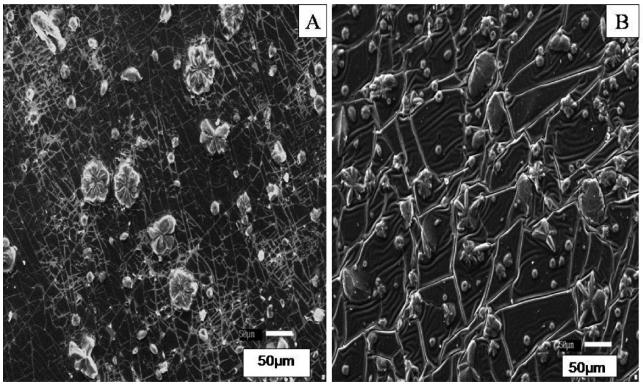

Figure 3. SEM image of gelatin with wt % of $LiClO_4$ as follows: (A) 14.63; (B) 16.67. The excess salt is seen to form aggregates.

sizes distributed irregularly. The salt aggregates probably block the paths for ion motion, and the conductivity falls off as shown later. It is not possible to measure the bond lengths for these images, and corresponding histograms cannot be shown.

3. ELECTRICAL PROPERTIES

3.1. Impedance Spectroscopy. HIOKI LCR meter 3532-50 was used to measure the complex impedance at room temperature (30 °C) in the frequency range 50 Hz to 2 MHz. The dc conductivity obtained from Cole−Cole plots is shown in Figure 4 as a function of salt fraction. The conductivity shows an initial peak, then falls before rising again to the highest peak at 12.5%, and then falls off slowly. We show the variation of real and imaginary parts of the impedance as functions of frequency for different salt fractions in Figures 5 and 6. Figures 7 and 8 show the results for salt fractions higher

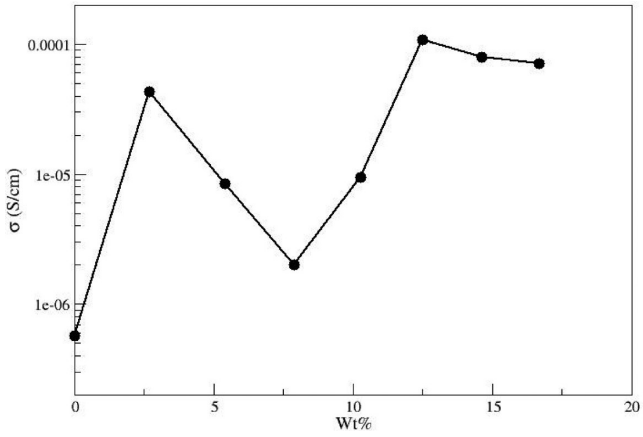

Figure 4. Variation in dc ion-conductivity with salt fraction at room temperature.

than 12.5%. All experimental results are compared with calculations from the theory described in section 4.

3.2. Direct Current as a Function of Time: Transference Number. A dc voltage was applied to the sample, and the current was measured as a function of time on a 2400 Source Meter (Keithley). The fall in current was monitored by video camera. The transference number was determined to be in the range 0.95−0.98, indicating predominantly ionic conduction in the samples. The graph of $I(t)$ vs t shown in Figure 9 illustrates the fall in current as polarization develops. We have calculated this as shown in subsequent sections and compared with the experimental curve.

4. THEORY

We follow the formalism developed by Lenzi et al.[14] This theory is developed for a liquid electrolyte, but we assume that it is applicable for a solid electrolyte as well. The ion-conduction mechanism in noncrystalline solid electrolytes is very similar to liquids, in particular for polymer samples above glass transition where dynamic disorder is present. Such materials, though apparently solid, are characterized by segmental motion, with parts of the macromolecular chain in incessant motion on very small spatial and temporal scales,[18] leaving the center of mass of the molecule stationary. However, this idea loses its validity when the salt fraction in the sample is so high that all the Li^+ ions cannot form a homogeneous complex. For salt fractions higher than 12.5%, SEM micrographs show that the salt forms aggregates, making the system inhomogeneous, and we find that agreement between the present theory and experimental results is no longer satisfactory.

We give the salient points of the theory in brief. The material consists of a uniform "solvent" with dimensionless, equally charged positive and negative ions moving with a certain mobility. The solvent is assumed to have an effective dielectric constant ϵ. The sample has surface area S and thickness d. The external field causes a local bulk density of positive (negative) ions represented by $\delta n_{\pm}$. Using the equation of continuity, the expression for current density, and the Poisson equation, one obtains the following equation

$$-{}_{-\infty}\mathcal{D}_t^{\gamma}\delta n_{\pm}(z,t) = D_{\gamma}\frac{\partial^2}{\partial z^2}\delta n_{\pm}(z,t) \pm \frac{NqD_{\gamma}}{k_B T}\frac{\partial^2}{\partial z^2}V(z,t) \quad (2)$$

dx.doi.org/10.1021/jp306205h | J. Phys. Chem. B 2012, 116, 11362−11369

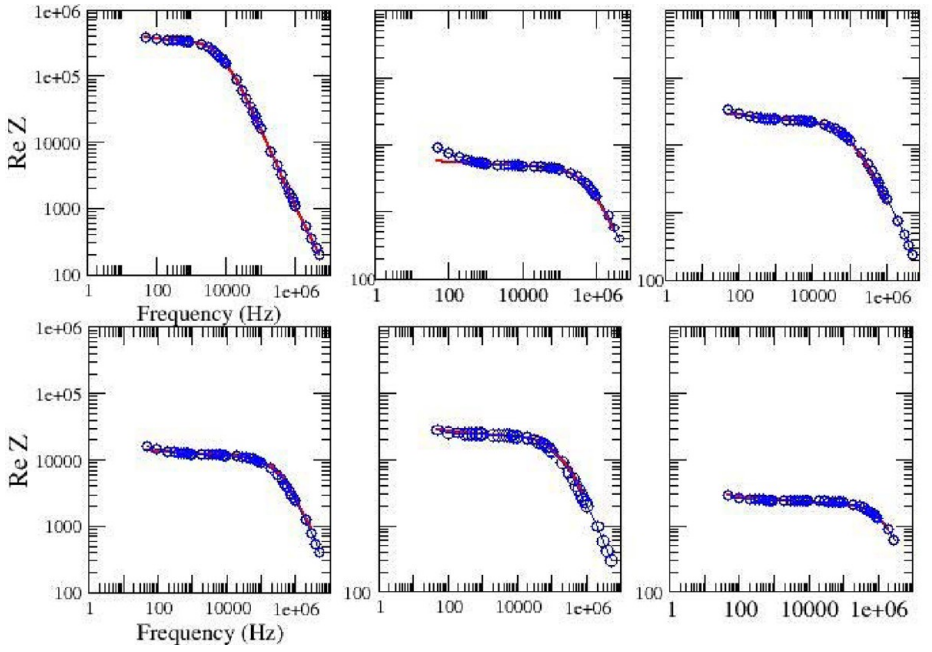

Figure 5. Real part of Z vs frequency (solid red line for theoretical value, blue circles for experimental values) with wt % of $LiClO_4$ varying from 0 to 12.5. x increases from left to right - upper row, then left to right - lower row.

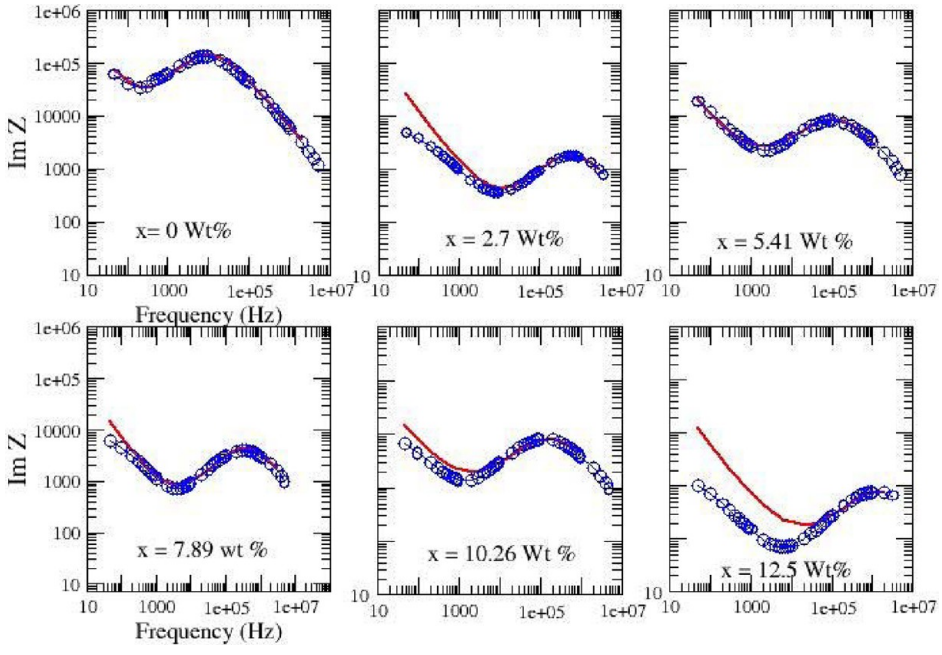

Figure 6. Imaginary part of Z vs frequency (solid red line for theoretical value, blue circles for experimental values) with wt % of $LiClO_4$ varying from 0 to 12.5. x increases from left to right - upper row, then left to right - lower row.

The first order time derivative in the equation of continuity has been replaced by the Riemann−Liouville fractional derivative[15] ${}_{-\infty}\mathcal{D}_t^{\gamma}$ of order γ for a mathematical description of anomalous diffusion. On the right-hand side, D_γ represents the diffusion coefficient and the second term is the drift term. N and q represent, respectively, the concentration of charge carriers and their charge. T is the absolute temperature. This equation2 can be solved to get an expression for the complex impedance $Z(\omega)$ in the case of anomalous diffusion.

However, the impedance involving only anomalous diffusion characterized by the fractional order γ does not give a realistic dispersion with frequency. We assume that a normal diffusion regime is present as well as the fractional diffusion. Introducing a contribution of h fraction of anomalous and $(1 - h)$ fraction of normal diffusion in the equation, the final expression for Z is obtained as

$$Z = \frac{2}{i\omega\epsilon S\beta^2}\left[\frac{1}{{\lambda_D}^2\beta}\tanh\left(\frac{\beta d}{2}\right) + h\frac{(i\omega)^{\gamma} d}{2D_\gamma} + (1 - h)\frac{i\omega d}{2D}\right] \quad (3)$$

dx.doi.org/10.1021/jp306205h | J. Phys. Chem. B 2012, 116, 11362−11369

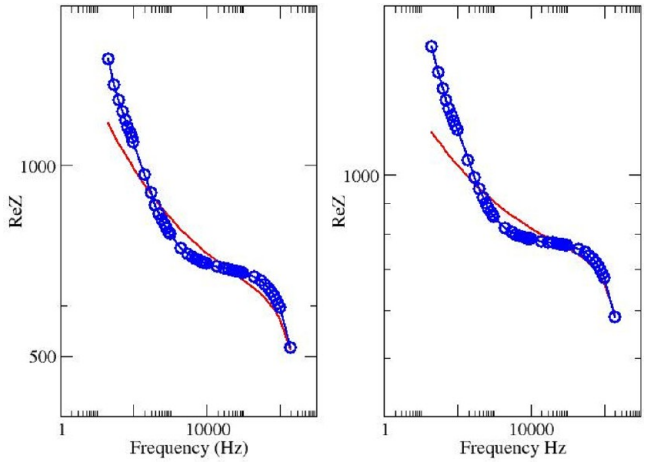

Figure 7. Real part of Z vs frequency (solid red line for theoretical value, blue circles for experimental values) for higher wt % of $LiClO_4$, 14.63% (left) and 16.67% (right).

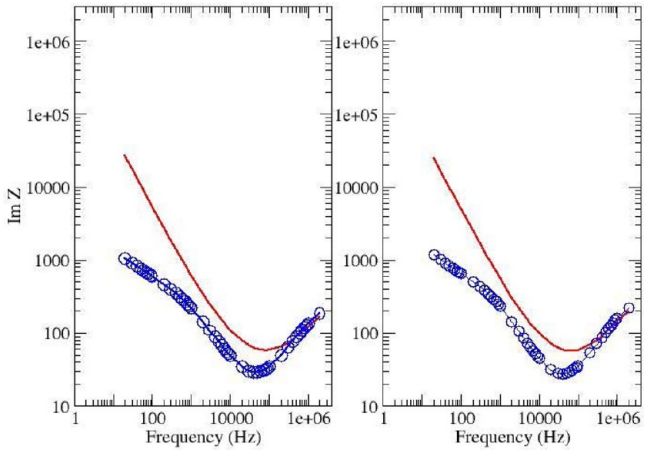

Figure 8. Imaginary part of Z vs frequency (solid red line for theoretical value, blue circles for experimental values) for higher wt % of $LiClO_4$, 14.63 (left) and 16.67 (right).

with β given by

$$\beta = \pm\sqrt{\frac{1}{\lambda_D{}^2} + h\frac{(i\omega)^\gamma}{D_\gamma} + (1-h)\frac{i\omega}{D}} \tag{4}$$

where λ_D is the Debye length defined as

$$\lambda_D = \sqrt{\frac{k_B \epsilon T}{2Nq^2}} \tag{5}$$

Equation 3 is used to interpret our experimental results for complex Z as a function of frequency for different salt fractions.

5. COMPARING THEORY AND EXPERIMENT

5.1. Impedance $Z(\omega)$ in Frequency Domain. The parameters in the expression for Z are determined as follows; we try to keep the number of adjustable parameters as small as possible. In the theory, ϵ is the dielectric constant of the continuum, hosting the mobile charge carriers. In this case, it is the effective dielectric constant of gelatin with glycerol and formaldehyde, which is the same for all samples irrespective of x. This is determined from the result for the $x = 0$ sample and henceforth assumed constant.

The mechanism of ion-conduction is described by the fractional diffusion equation with order γ. The value of γ may however vary with salt fraction as the morphology (seen from SEM) and charge distribution within the material changes. We have allowed γ to vary; however, the final values shown in Table 1 are all quite close to 0.8. The results are highly sensitive to γ, and the fits in Figures 5 and 6 worsen considerably if γ is set to a common value for all x. The noticeable feature is that for the salt free sample γ is 0.86, closer to the value 1 for normal diffusion.

The crucial feature here is the relative importance of the anomalous diffusion in comparison to normal diffusion, which we find to change with x. The fractional contribution of anomalous diffusion h and γ both characterize this. h may arguably vary with x. However, we keep it constant here to avoid too many free fitting parameters. This should not matter too much, as the deviation from normal diffusion is partly taken care of by γ.

The diffusion coefficients corresponding to normal and anomalous diffusion D and D_γ are the truly free parameters in this formalism.

Now all parameters are adjusted to give a best fit to the experimental curves for Z(real) and Z(imaginary) as a function of frequency. The input parameters, namely, the film thickness d and the calculated Debye length λ_D as well as the best fit free parameters for all the samples are given in Table 1.

Another parameter is necessary to calculate the Debye length λ_D for different x. The charge carrier concentration N in the expression for λ_D is the sum of the ion concentration for $x = 0$ and the additional ions for nonzero x. We determine $N(x = 0) = 0.5 \times 10^{20}/m^3$ from the best fit to experimental $Z(\omega)$ for $x = 0$ and add the effective number of charge carriers, i.e., Li^+ ions. The total number of ions $N_{salt}(x)$ comes out to be of the order $10^{27}/m^3$. If all these ions participate equally in the conduction process, the calculated conductivity would exceed the observed value by several orders of magnitude. It is well-known that all ions in a polymer electrolyte do not contribute to the conduction process.[1,3] Interaction between ions causes charge immobilization and often ion aggregates formed by multiple ions have insignificantly small mobility. Thus, we have to introduce a reduction factor which gives the effective number of Li^+ ions to be taken into account.

We assign an effective value to the reduction factor which gives a realistic magnitude to the conductivity. This factor is assumed to be 5.056×10^{-7} and to remain the same for all x. An effective number of Li^+ ions of the order $10^{21}/m^3$ is not unreasonable considering earlier estimates[19] of lithium ion concentration in PEO to be $\sim 10^{27}/m^3$ at much higher temperatures near 150 °C. Thus, N is given by

$$N = N_{(x=0)} + 5.056 \times 10^{-7} \cdot N_{salt}(x) \tag{6}$$

λ_D calculated thus for different x are tabulated in Table 1. h and ϵ are kept constant for all x, so the only remaining "free" parameters are γ (which is between 0.86 and 0.79) and the diffusion coefficients, these are adjusted to give the best fit to experimental data for varying x and are listed in Table 1. Figures 5 and 6 show the theoretically calculated curves compared with experiments.

The samples with x higher than $x = 12.5\%$ do not fit well into this scheme; these results are shown in Figures 7 and 8. The calculated curves for Z(real) and Z(imaginary) against frequency show a strong deviation from experiment. It seems

dx.doi.org/10.1021/jp306205h | J. Phys. Chem. B 2012, 116, 11362−11369

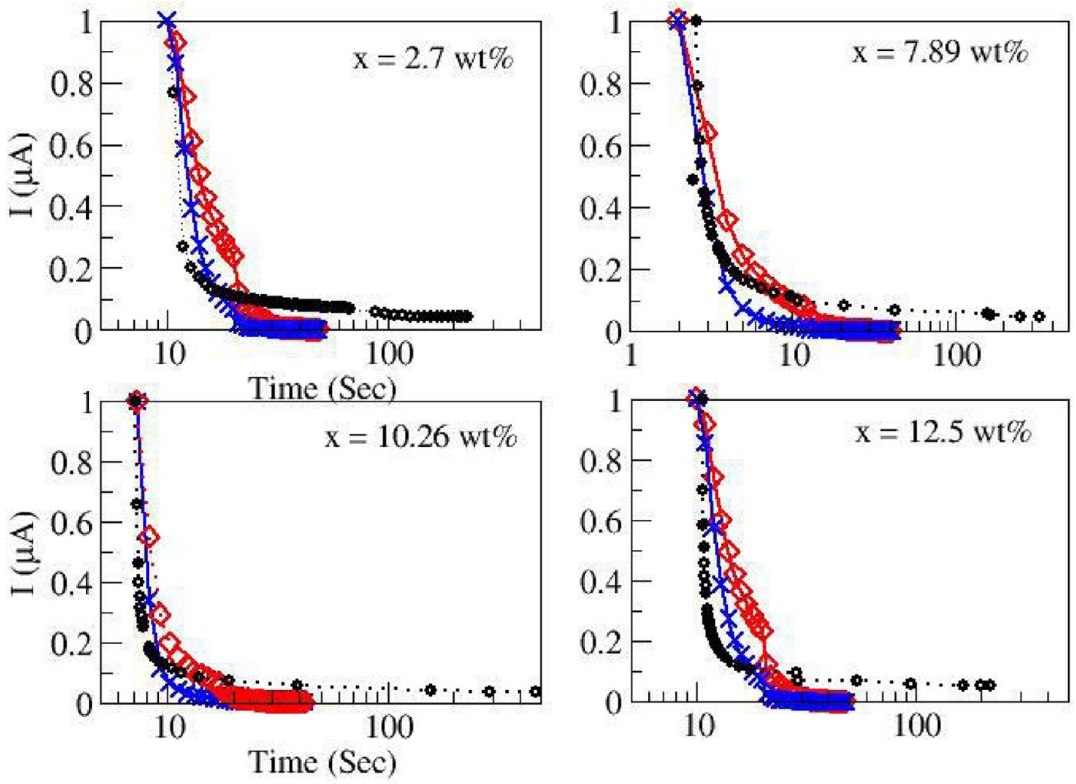

Figure 9. Result for time domain. Blue crosses and red diamonds show, respectively, the real part and the modulus of the current I calculated from eq 7, and black lines with black circles show experimental values, for 2.70, 7.89, 10.26, and 12.50 wt % $LiClO_4$.

Table 1. Experimental Input Parameters and Best Fit Model Parameters for Samples with Varying x

salt conc. (%)	thickness (d, μm)	λ_D (μm)	ϵ	h	γ	D_γ (10^{-7} m^2/s)	D (10^{-5} m^2/s)
0.00	387	2.2060	340	0.634	0.862	0.457	4.70
2.70	375	0.8926	340	0.634	0.840	1.838	60.06
5.41	388	0.6441	340	0.634	0.817	0.160	6.55
7.89	340	0.4908	340	0.634	0.811	0.230	6.90
10.26	351	0.4330	340	0.634	0.793	0.074	2.80
12.50	310	0.4257	340	0.634	0.800	0.470	28.80

that the theory is inadequate for a heterogeneous sample where salt aggregates shown in Figure 3 hinder ion-conduction.

5.2. $I(t)$ in Time Domain. We can invert the frequency domain results to get time variation of current under constant voltage. Assuming that a steady voltage of 1 V is applied at t = 0, we can calculate $I(t)$ as follows. The expression for $Z(\omega)$ is convoluted with the Heaviside step function, and the inverse Laplace transform gives the current as

$$I(t) = \mathcal{L}^{-1}\frac{1}{j\omega Z(\omega)} \tag{7}$$

Figure 9 compares the calculated curve from this equation with parameters from Table 1 and the experimentally measured current (using 2400 Source Meter, Keithley) for several different x where the ion-conductivity is high. The initial values for both curves are normalized to 1. The experimental curve is slightly shifted to the right for a better fit. This is permissible, since it accounts for a possible delay in capturing the initial moment on video. The experimental curves are smoother and fall off more slowly. The theory assumes a zero dc conductivity, which may not be realized exactly in practice. The calculated curves have a slight kink and fall rapidly to zero, but the overall agreement is acceptable.

6. DISCUSSION

We have studied the morphology and impedance behavior of a gelatin based solid polymer electrolyte and find a considerable increase of dc ion-conductivity with lithium perchlorate concentration. The ion-conductivity first rises by nearly 2 orders of magnitude as the salt is introduced in the plasticized gelatin host and then falls slightly and rises again to the highest peak at x = 12.5%. Earlier measurement at a higher temperature showed a decrease in σ at x = 12.5% with a peak at x = 10.26%.[20] Occurrence of double peaks in σ as x varies is a familiar observation in several polymeric and biopolymer materials.[12,13] We see from both of the diffusion coefficients in Table 1 that they have two peaks in accordance with the conductivity variation. However, the second peak in diffusivity values is much lower than the first. This may be interpreted as follows. Two factors contribute to ion-conduction; one is the *concentration* of charge carriers, and the other is their *mobility*. The first peak in conductivity (x = 2.7 wt %) occurs when a small number of carriers are introduced, but their mobility is

dx.doi.org/10.1021/jp306205h | J. Phys. Chem. B 2012, 116, 11362−11369

very high, due to the favorable open morphology with the less dense network. The second peak is dominated by the large number of carriers (with increased x = 12.5%), though the mobility is not so high. This is reflected in the values of D and D_γ, which are high but not as high as for x = 2.7%. Thus, the competition between the charge carrier concentration and their mobility, determined by the microstructure, is responsible for the complicated variation in ion-conductivity.

The other principal motivation of this work is to demonstrate the usefulness of the fractional diffusion approach, involving material properties, to develop a better understanding of the microscopic processes at work in a solid ion conductor. A standard fitting procedure using an equivalent circuit with lumped elements and CPEs provides relatively little insight into the basics of the system.

We have incorporated a normal diffusion component as well as an anomalous diffusion process into the model. Let us review the implications of the best fit parameter values listed in Table 1. The Debye length λ_D depends on the salt fraction and decreases monotonically with increasing x. The parameters obtained for x larger than 12.5% are not given, as the fit to experiments (Figures 7 and 8) is not acceptable and shows that as the system becomes inhomogeneous the theory fails.

The relative contributions from the normal and anomalous diffusion processes, given by the parameter h = 0.634, show that both are equally important. The parameter γ which is the order of the fractional derivative involved takes the value ~0.8 for all x studied. This is quite different from the value γ = 1 corresponding to normal diffusion. The importance of anomalous diffusion in polymer ion-conductors, arising from the fractal structure of polymers, has been discussed in several earlier works.[21,3] The two diffusion coefficients corresponding to normal and anomalous diffusion differ by 2 orders of magnitude, but both follow the variation of the σ curve in Figure 4, increasing when the ion-conductivity increases, as expected. The relatively lower diffusivities at the second peak compared to the first explain the effect of reduced mobility, but the conductivity is highest here as the concentration x plays a more dominant role. The anomalous diffusion coefficient $D_\gamma < D$ and being in the denominator contribute strongly to Z.

The real and imaginary parts of the calculated impedance $Z(\omega)$ both agree remarkably well with the experimental results up to x = 12.5%, except for the low frequency ends for Z(Im) in two cases. However, for higher salt fractions, where Figure 3 shows salt aggregation, the Z(imaginary) curve does not agree well with the calculation, particularly at low frequencies. The number of free parameters is very small compared to the amount of data points calculated. The parameters ϵ and h have been kept fixed for all x, since ϵ represents the host material and h characterizes the system. γ has been allowed to vary, but it never deviates much from 0.8. Thus, finally, D and D_γ are the principal fitting parameters for Z(Re) and Z(Im) for the different salt fractions studied.

It is important to note that the normal and anomalous diffusion both play an important role and neither can be neglected to explain the impedance results properly. The work of McDonald et al.[22] compares the formulation by Lenzi et al.[14] with other models and finds some inconsistencies in the approach followed here. However, the unphysical behavior of the admittance Cole−Cole plot shown there for interface conduction is not observed here; we show the plot for x = 7.89 and 10.26 wt % in Figure 10 to clarify this.

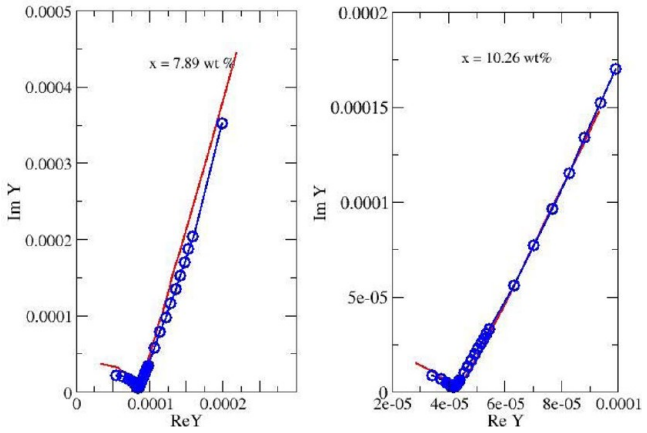

Figure 10. Plot for Y(Im) vs Y(Real) from the theoretical calculation (red line) compared with the experimental values (blue circles and lines) for x = 7.89 and 10.26 wt %.

The morphology seen from the SEM images in Figure 1 shows that for the samples with high conductivity the polymer chain strands form a sparse and loose network, compared to the dense network in other cases. Probably, this indicates easy segmental motion enhancing ion-conduction. It may be conjectured that a rigid and dense polymer network inhibits ion motion. Another interesting fact is that the bond length distribution in the SEM images follows a log-normal distribution for the samples with salt where the ion-conductivity is low but follows a symmetric normal (Gaussian) distribution in the other cases where conductivity is high. Probably the predominance of short bonds in the log-normal distribution is indicative of the rigidity of the network, preventing easy motion of ions. The distribution is also symmetric for the x = 0 case, but here of course conductivity is low, as there are no lithium ions. We cannot offer an explanation for this right now, but it may be a topic for future study.

To conclude, biopolymers are a promising class of materials for providing cost-effective and environment friendly technology. Further, to analyze such materials, an approach based on a physical model is preferable to curve fitting exercises involving many parameters which cannot be interpreted physically. The concept of fractional diffusion provides a useful tool to study these complex systems.

AUTHOR INFORMATION

Corresponding Author

*E-mail: sujata_tarafdar@hotmail.com, sujata@phys.jdvu.ac.in. Phone: +91 33 24146666 (ext. 2760). Fax: +91 33 24148917.

Notes

The authors declare no competing financial interest.

ACKNOWLEDGMENTS

The authors are very grateful to Mrs. S. Roy, Senior technical officer, C.G.C.R.I., Kolkata. The authors sincerely thank Partha Pratim Roy, Animesh Layek, and Somnath Middya, Jadavpur University, for help with experiments and Shantanu Das for stimulating discussion on fractional calculus. T.B. thanks DST, Govt. of India, for award of INSPIRE research fellowship.

REFERENCES

(1) Vincent, C. A. *Prog. Solid State Chem.* **1987**, *17*, 145−261.

(2) Armand, M. *Solid State Ionics* **1994**, *69*, 309−319.
(3) Gray, F. M. *Solid Polymer Electrolytes*; VCH: New York, 1991.
(4) Tiwari, T.; Srivastava, N.; Srivastava, P. C. *Ionics* **2011**, *17*, 353−360.
(5) Tiwari, T.; Pandey, K.; Srivastava, N.; Srivastava, P. C. *J. Appl. Polym. Sci.* **2011**, *121*, 1−7.
(6) Mattos, R. I.; Pawlicka, A.; Tombelli, C. E.; Donoso, J. P. *Mol. Cryst. Liq. Cryst.* **2008**, *483*, 120−129.
(7) Mattos, R. I.; Pawlicka, A.; Lima, J. F.; Tombelli, C. E.; Magon, C. J.; Donoso, J. P. *Electrochim. Acta* **2010**, *55*, 1396−1400.
(8) MacCallum, J. R.; Smith, M. J.; Vincent, C. A. *Solid State Ionics* **1984**, *11*, 307−312.
(9) Karmakar, A.; Ghosh, A. *Phys. Rev. E* **2011**, *84*, 051802−051808.
(10) Karmakar, A.; Ghosh, A. *Curr. Appl. Phys.* **2012**, *12*, 539−543.
(11) Godjourova, Z.; Andreev, Y. G.; Tunstall, D. P.; Bruce, P. G. *Nature* **2001**, *412*, 520−3.
(12) Reddy, P.; Kumar, A. R.; Causin, V.; Neppalli, R. *J. Korean Phys. Soc.* **2011**, *59*, 114−118.
(13) Kumar, M.; Tiwari, T.; Srivastava, N. *Carbohydr. Polym.* **2012**, *88*, 54−60.
(14) Lenzi, E. K.; Evangelista, L. R.; Barbero, G. *J. Phys. Chem. B* **2009**, *113*, 11371−11374.
(15) Das, S. *Functional fractional Calculus*, 2nd ed.; Springer: Berlin, 2011.
(16) Ribeiro, H. V.; Rossato, R.; Tateishi, A. A.; Lenzi, E. K.; Mendes, R. S. *Acta Sci., Technol.* **2012**, *34*, 201−206.
(17) Crow, E. L.; Shimizu, K. *Log Normal Distributions: Theory and Applications*; Marcel Dekker: New York, 1988.
(18) Ratner, M. A.; Nitzan, A. *Solid State Ionics* **1988**, *28−30*, 3−33.
(19) Bhattacharja, S.; Smoot, S. W.; Whitmore, D. H. *Solid State Ionics* **1986**, *18/19*, 306−308.
(20) Basu, T.; Goswami, M. M.; Middya, T. R.; Tarafdar, S. *Proceedings of the 9th National Conference on Solid State Ionics*, Noida, India, 2011.
(21) Maitra, M.; Mal, D.; Dasgupta, R.; Tarafdar, S. *Physica A* **2004**, *346*, 191−199.
(22) Macdonald, J. R.; Evangelista, L. R.; Lenzi, E. K.; Barbero, G. *J. Phys. Chem. C* **2011**, *115*, 7648−7655.